Table S1 Data collection and refinement statistics

	Srx−PrxI Complex
Data collection	
Space group	$P2_12_12_1$
Cell dimensions	
a, *b*, *c* (Å)	54.9, 85.0, 130.8
α, β, γ (°)	90, 90, 90
Resolution (Å)	51.85 – 2.60 (2.67 – 2.60 Å)*
R_{sym}	6.2 (38.5)
$I/\sigma I$	15.8 (4.7)
Completeness (%)	100 (100)
Redundancy	6.9 (7.0)
Refinement	
Resolution (Å)	51.85 – 2.60
No. reflections (work/free)	18499/995
R_{work}/R_{free}	0.233/0.303
No. atoms	
Protein	4459
Water	10
B-factors	
Protein	52.0
Water	39.2
R.m.s deviations	
Bond lengths (Å)	0.013
Bond angles (°)	1.549
Ramachandran analysis (%)	
favored regions	94.5
allowed regions	4.9
outlier	0.6

*Highest resolution shell is shown in parenthesis.

Supplemental Figures

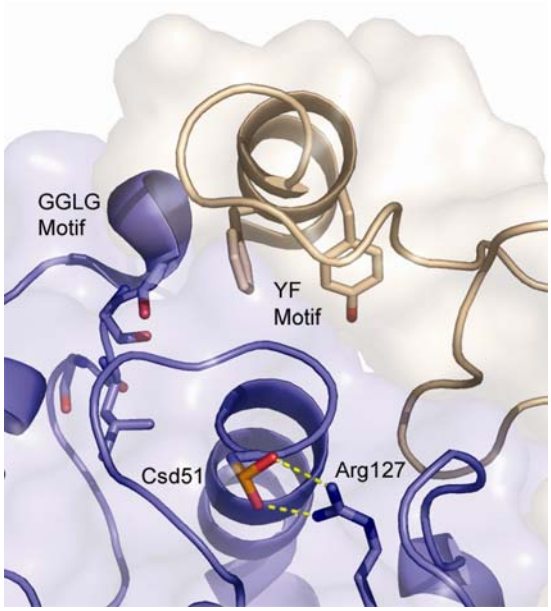

Figure S1 | Inaccessibility of the hyperoxidized active site of human PrxII. A close-up view of one hPrxII active site (blue surface and ribbon) illustrates the difficulty Srx has in gaining access to the Cys51-$S_PO_2^-$ moiety (Csd51). This residue is involved in a salt bridge interaction with Arg127. The Prx active site is occluded primarily by residues of the YF motif within the C-terminal α-helix of the adjacent Prx molecule (tan surface and ribbon). This latter structural feature also interacts with the GGLG motif to promote hyperoxidation of 2-Cys Prxs.

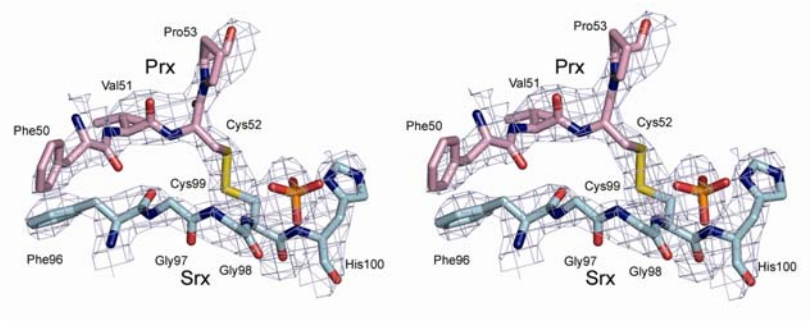

Figure S2 | The engineered disulfide bond of the Srx–PrxI complex. Simulated-annealing omit $2F_o$-F_c electron density map (grey) contoured at 1σ. Residues 50-53 of PrxI (violet) and 96-100 of Srx (cyan) are shown. A phosphate ion is coordinated by His100.

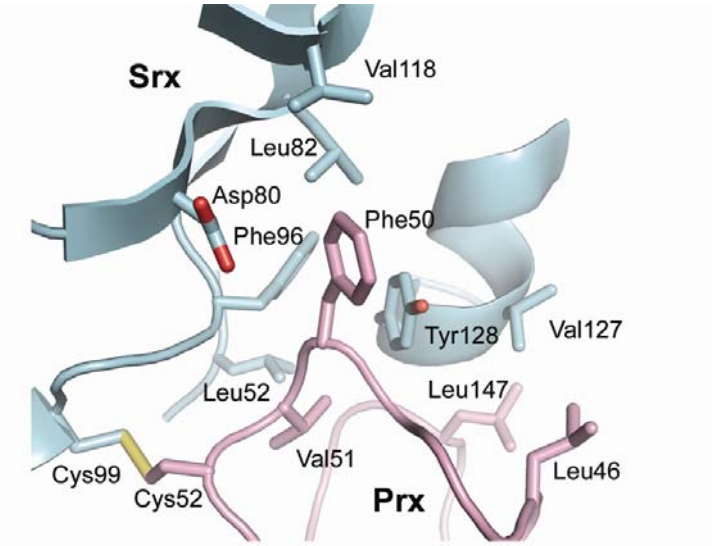

Figure S3 | Srx–PrxI active site interface near the engineered disulfide bond. Phe50 in PrxI (violet) interacts with a hydrophobic pocket in Srx (cyan) formed by Leu52, Asp80, Leu82, Phe96, Val118 and Tyr128. Residues Leu46, Phe50, Val51 and Leu147 of PrxI further complement the interaction.

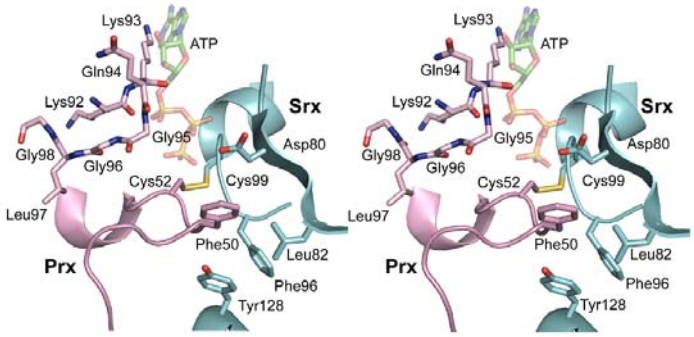

Figure S4 | Stereo image of ATP modelled (translucent) into the active site of the Srx-PrxI complex.

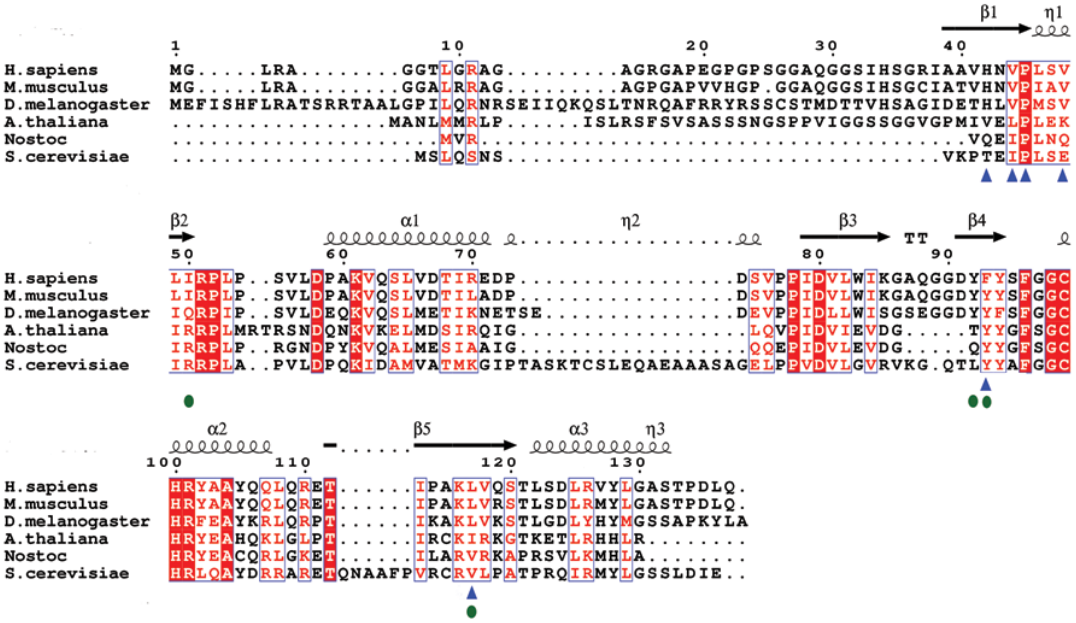

Figure S5 | Sequence alignment of representative sulfiredoxins. The Srxs from mouse, *Drosophila*, *Arabidopsis*, *Nostoc* species PCC7120, and *S. cerevisiae* show 91%, 60%, 43%, 41%, 33% sequence identity to hSrx, respectively. The secondary structural elements and residue numbers for human Srx are shown above the alignment: α, α-helix; β, β-strand; η, 3_{10} helix. The residues highlighted by the red background and white lettering are strictly conserved. Residues that are either conserved in the

majority of the proteins or have conservative substitutions are boxed in blue and colored red. The blue triangles indicate residues on the backside of Srx involved in the interaction with the C-terminal tail of PrxI. Green ovals indicate the residues which were mutated and analyzed in the fluorescence anisotropy and activity studies.

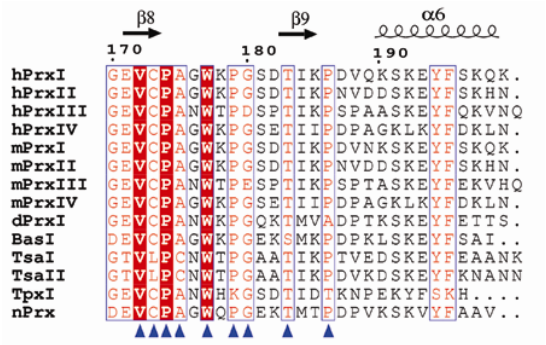

Figure S6 | Sequence alignment of the C-termini of representative 2-Cys Prxs sensitive to hyperoxidation. The 2-Cys Prx sequences shown are human PrxI-IV, mouse PrxI-IV, *Drosophila* PrxI, *Arabidopsis thaliana* BasI, *Saccharomyces cerevisiae* TsaI and TsaII, *Schizosaccharomyces pombe* TpxI, and *Nostoc* Prx. Secondary structure elements for hPrxII in the hyperoxidized form are indicated above the alignment : α, α-helix; β, β-strand. Blue triangles indicate residues in hPrxI that bind to the surface of Srx. The residue numbers at the top of the alignment are for hPrxI.

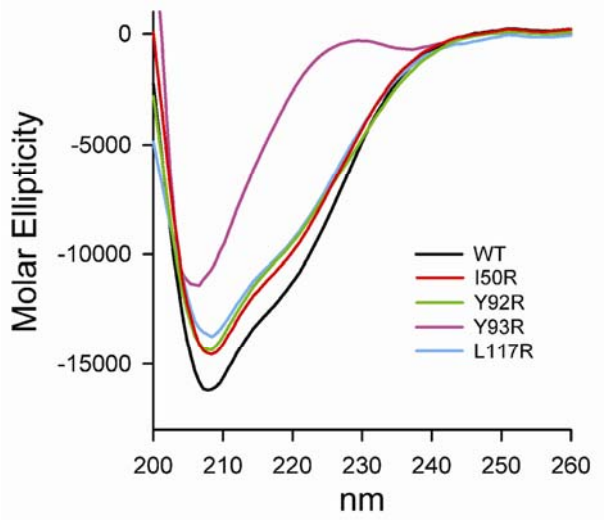

Figure S7 | CD spectra of wild-type and mutant Srx variants.

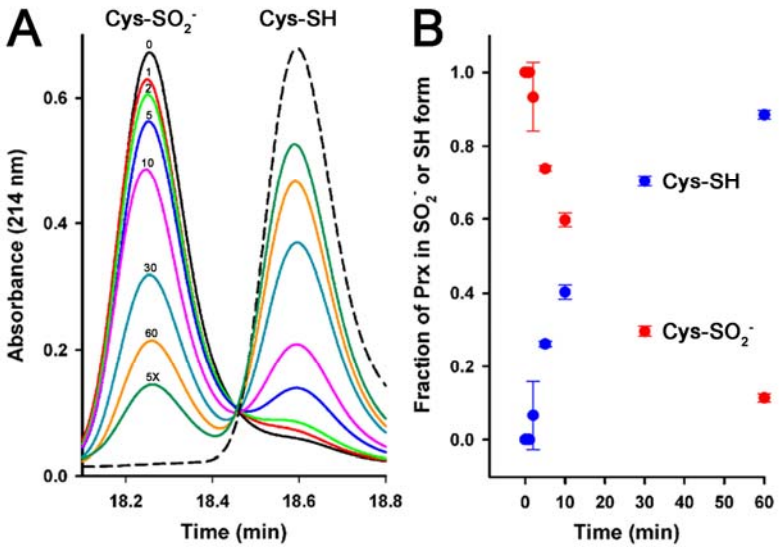

Figure S8 | HPLC analysis of the repair of decameric hPrxI-SO_2^- by Srx. a, PrxI-SO_2^- (solid black line) and PrxI-SH (black dashed line) standards were eluted from a C4 reverse-phase column with monitoring at 254 nm. The Srx reaction was initiated by

mixing 50 μM PrxI-SO_2^-, 10 μM wild-type ET-hSrx, 1 mM ATP, 1 mM $MgCl_2$, and 2 mM DTT. After incubation at 37 °C for the indicated incubation period, the samples were quenched by the addition of H_3PO_4 and analyzed. A 60 min reaction was also carried out in the presence of five-fold excess of Srx (250 μM, dark green) over PrxI-SO_2^-. Representative traces from duplicate runs. **b**, Fractional disappearance of PrxI-SO_2^- (red) and appearance of PrxI-CysSH (blue) as determined from the integrated HPLC chromatograms; representative data and s.d. of two independent reactions are shown. The Prx species that was irreparable, as determined by the reaction containing the five-fold (5X) excess of Srx, is most likely PrxI-SO_3^-.

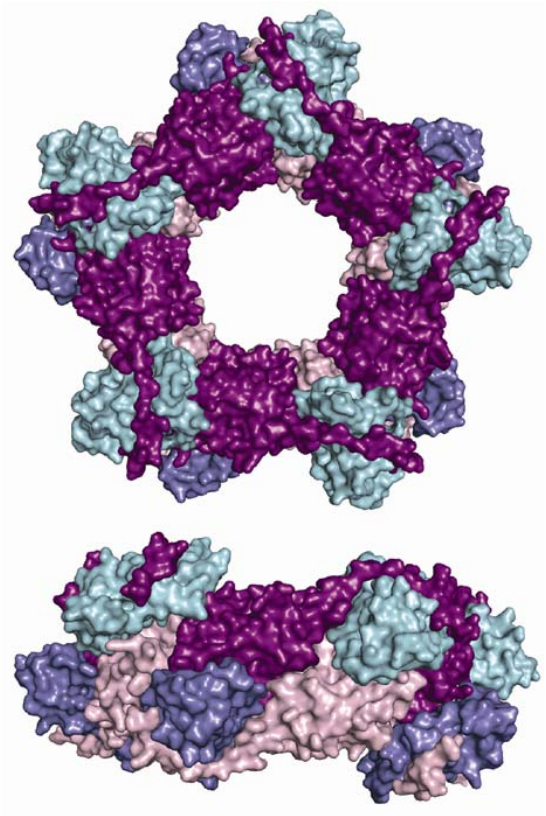

Figure S9 | Front and side views of the surface model of the decameric Srx–PrxI complex. At this time it is unclear if such a "fully-loaded" Srx–Prx complex exists *in vivo*, although this species can be generated *in vitro* (see Supplemental Methods).